Journal Name RSCPublishing

Dinuclear uranium complexation and manipulation using robust tetraaryloxides

Jordann A. L. Wells,[a] Megan L. Seymour,[a] Markéta Suvova,[a] and Polly L. Arnold[a*]

Contents

Compound numbering scheme 1

Additional Experimental details 1

K_4L^M 1

Selected NMR spectra 2

Selected cyclic voltammograms 9

Crystallographic details 11

Selected solid-state structure drawings 15

Compound numbering scheme

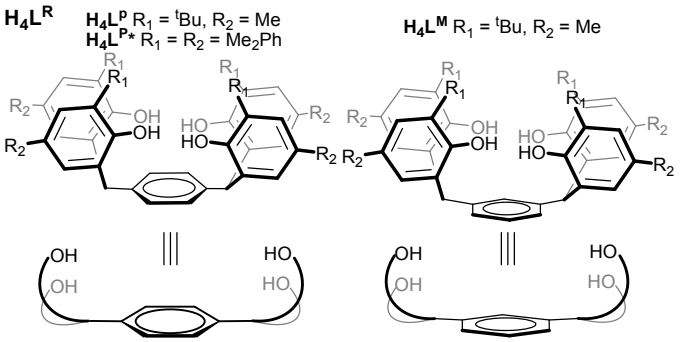

Figure S0 The substituted tetraphenols H_4L^P, H_4L^M and the aryl-substituted H_4L^{P*}, and their cartoon representations.

Additional Experimental details

K_4L^M

A Schlenk flask was charged with H_4L^M (2.00 g, 2.65 mmol) and KN" (2.11 g, 10.60 mmol) and equipped with a stirrer bar. THF was added and the resulting yellow solution was stirred for 16 hours at room temperature. Hexane was subsequently added to precipitate the product as a colourless powder which was isolated by filtration and dried under vacuum.

^{1}H NMR (d_8-THF, 329 K, 500 MHz) δ 7.45-6.92 (Aryloxide H, m, 4H), 6.78-6.59 (Aromatic H and Aryloxide H, m, 8H) 5.80 (Trityl H, s, 2H), 2.03 (MeH, s, 12H), 1.32 (tBu H, s, 36H).
Mass Spectrometry: (MALDI) m/z 907.601 [K_4L^M].

Selected NMR spectra

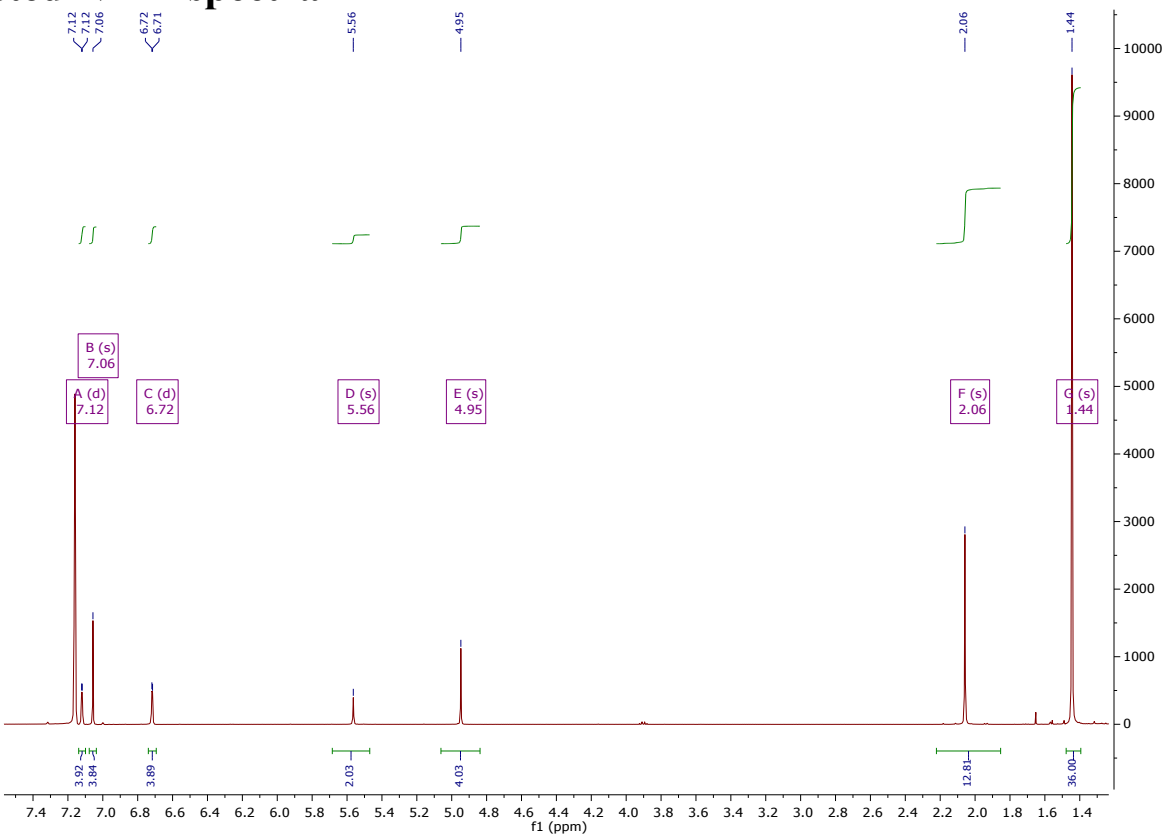

Figure S1 ^{1}H NMR spectrum of $\mathbf{H_4L^p}$ (C_6D_6, 500 MHz).

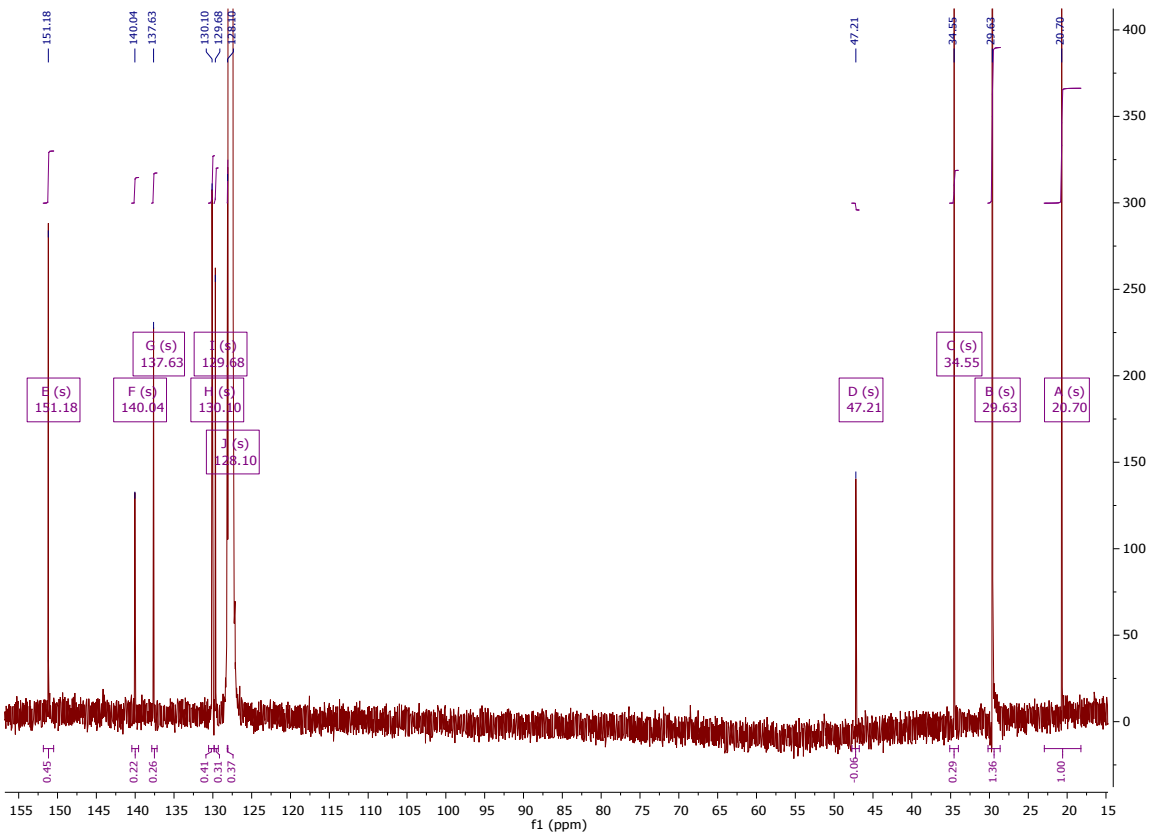

Figure S2 ^{13}C NMR spectrum of $\mathbf{H_4L^p}$ (C_6D_6, 126 MHz).

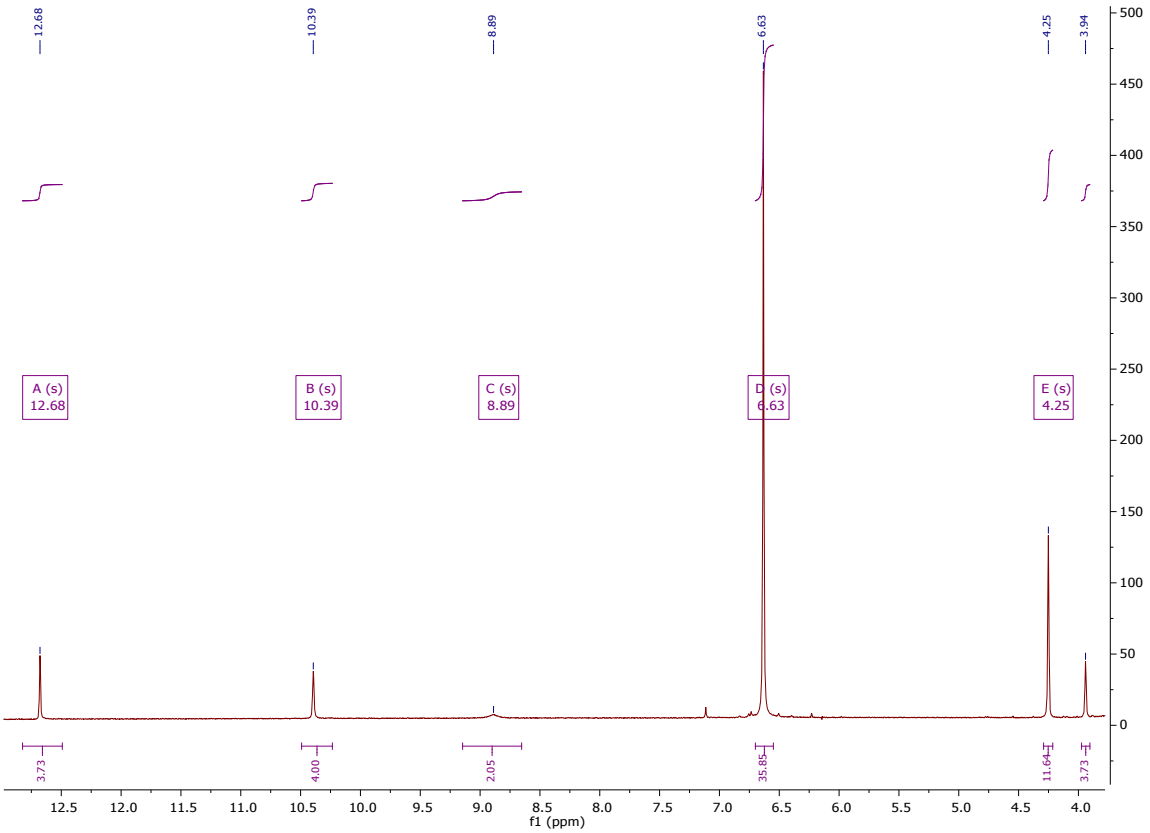

Figure S3 ^{1}H NMR spectrum of **1^{P} ($U_2I_4L^{P}$)** (d_8-THF, 329K, 500 MHz).

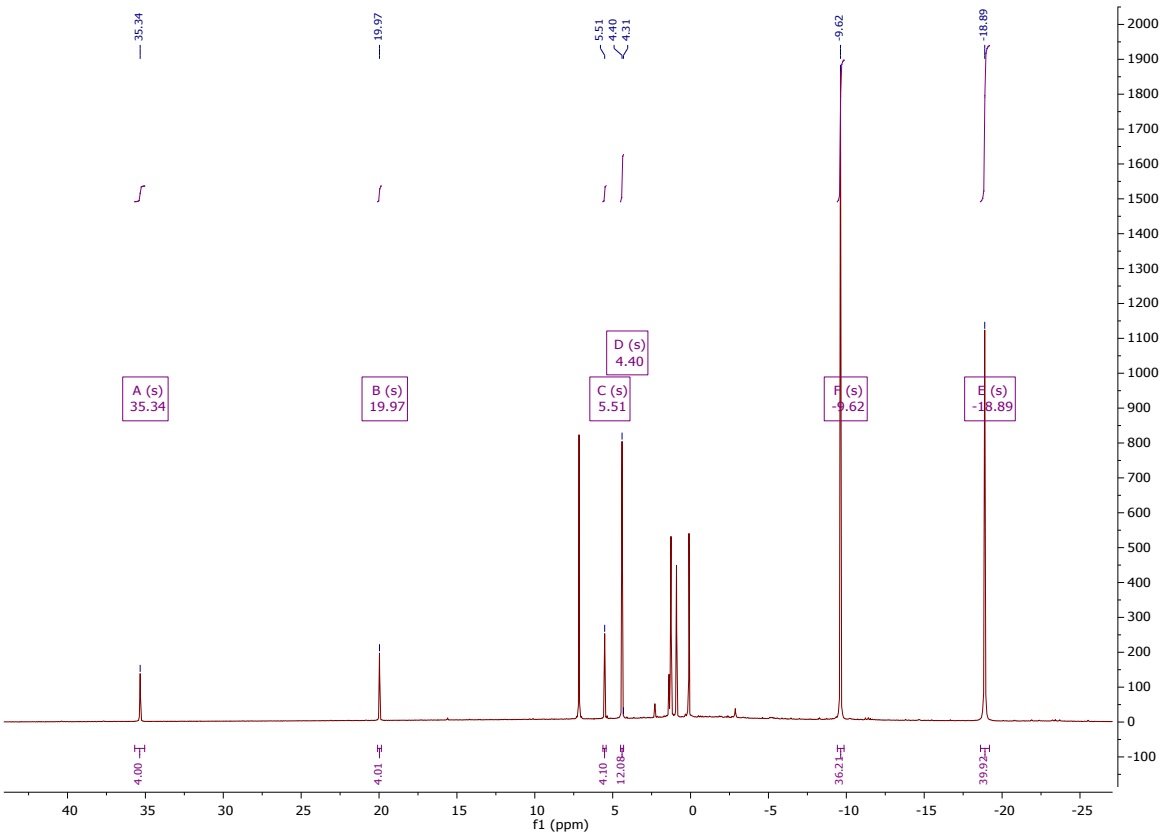

Figure S4 ^{1}H NMR spectrum of **2^{P} ($U_2N''_4L^{P}$)** (C_6D_6, 500 MHz).

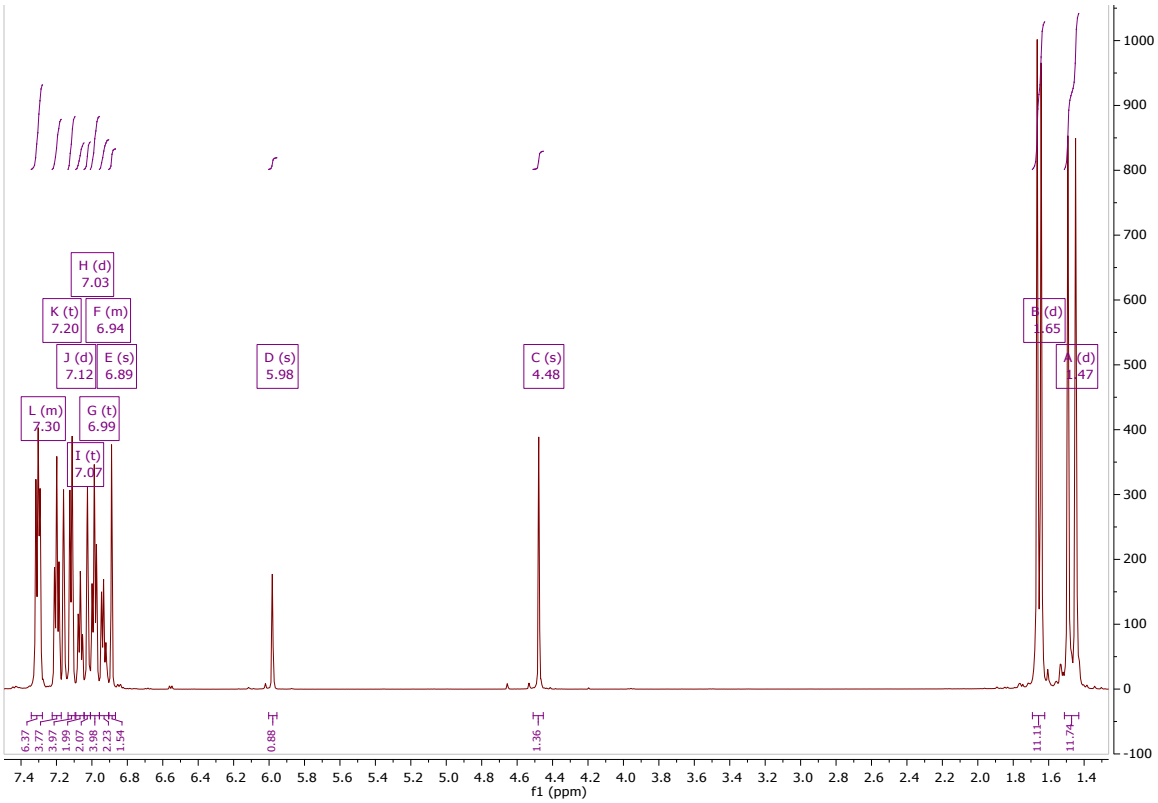

Figure S5 ^{1}H NMR spectrum of $\mathbf{H_4L^{P*}}$ (C_6D_6, 500 MHz).

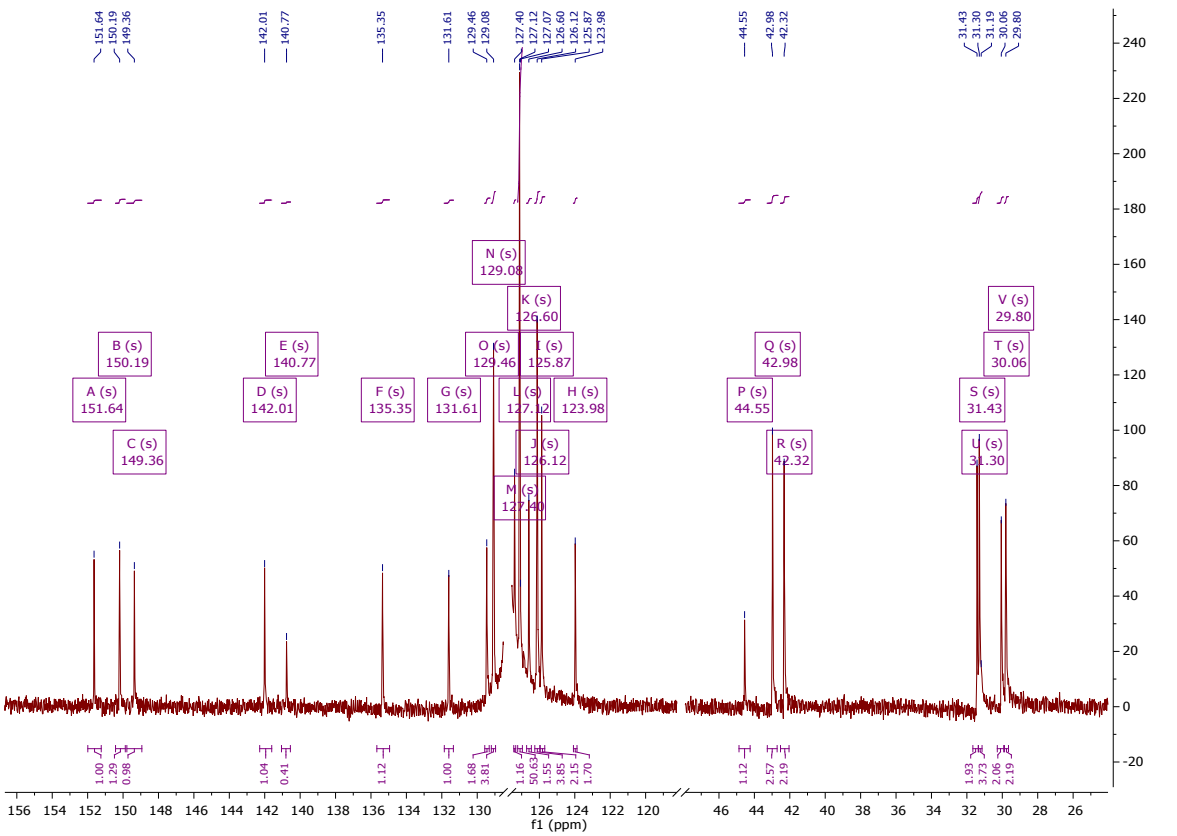

Figure S6 ^{13}C NMR spectrum of $\mathbf{H_4L^{P*}}$ (C_6D_6, 126 MHz).

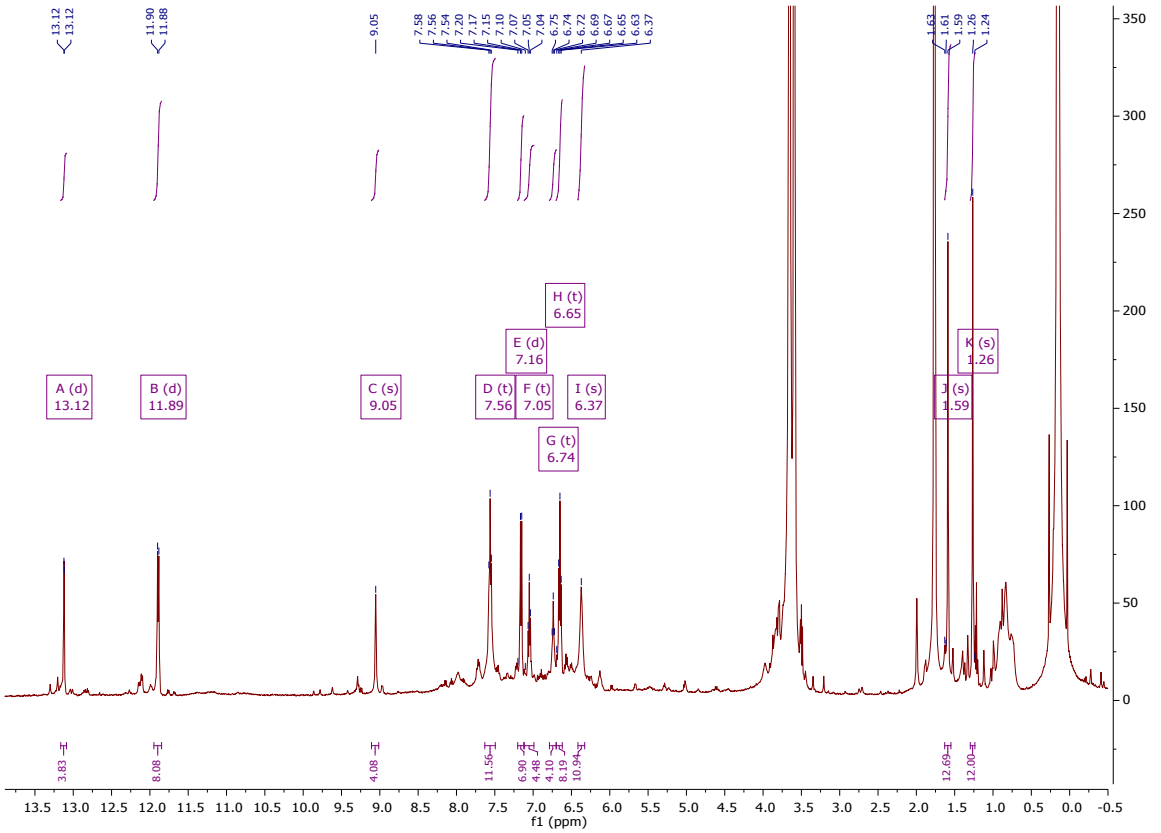

Figure S7 ^{1}H NMR spectrum of **1^{P*} ($U_2I_4L^{P*}$)** (C_6D_6, 500 MHz).

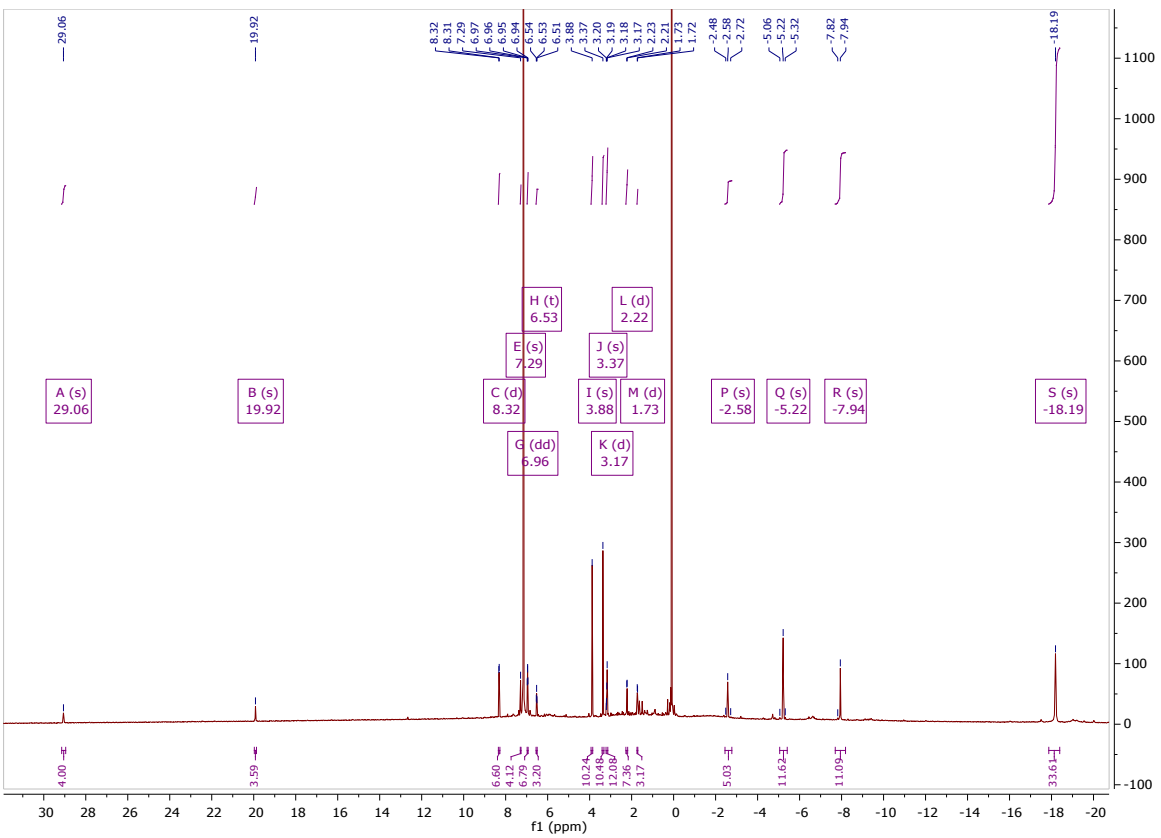

Figure S8 ^{1}H NMR spectrum of **2^{P*} ($U_2N''_4L^{P*}$)** (C_6D_6, 345 K, 500 MHz).

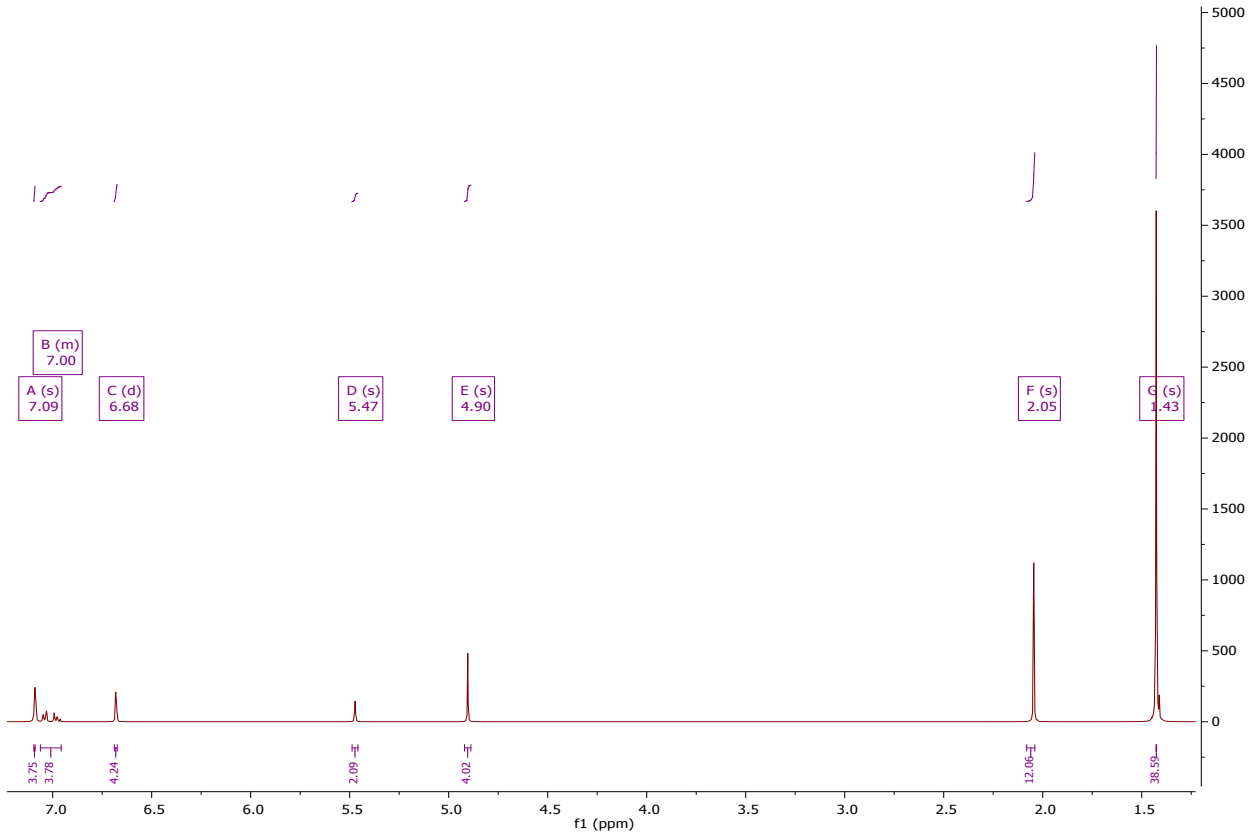

Figure S9 ^{1}H NMR spectrum of $\mathbf{H_4L^M}$ (C_6D_6, 500 MHz).

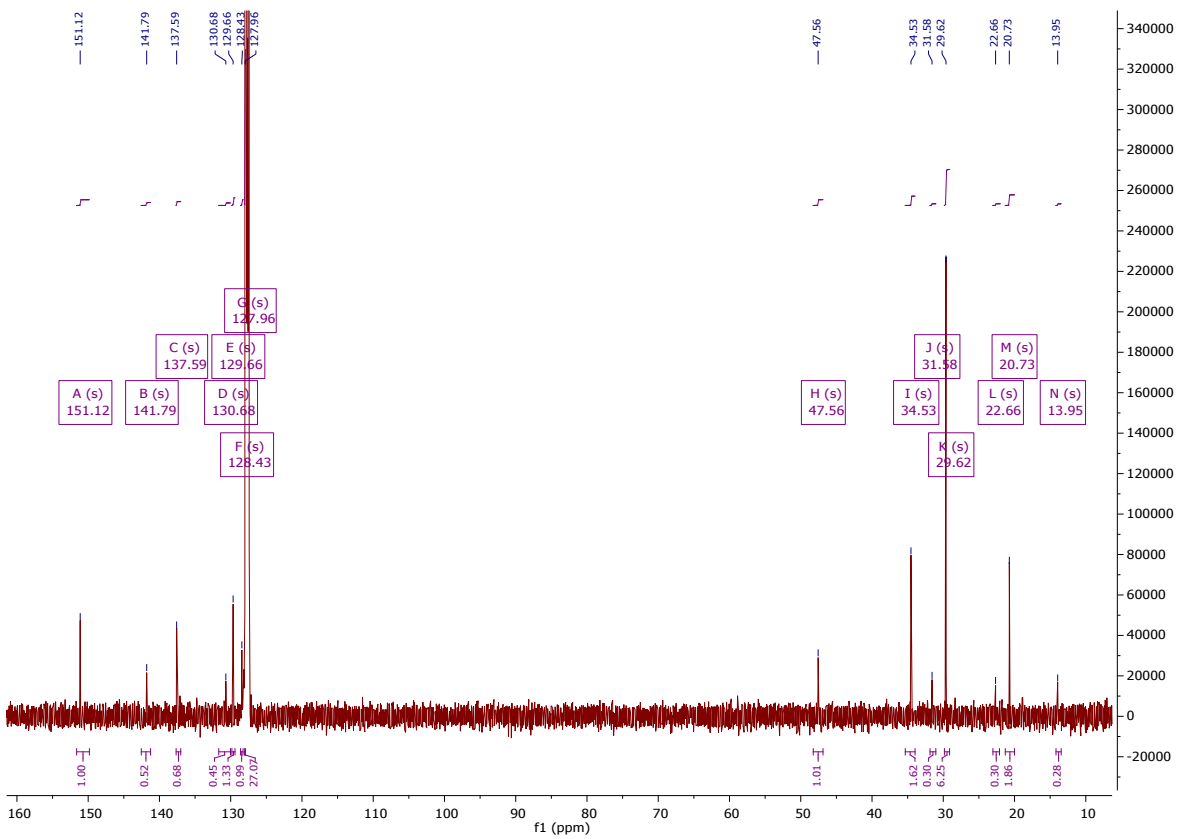

Figure S10 ^{13}C NMR spectrum of $\mathbf{H_4L^M}$ (C_6D_6, 126 MHz).

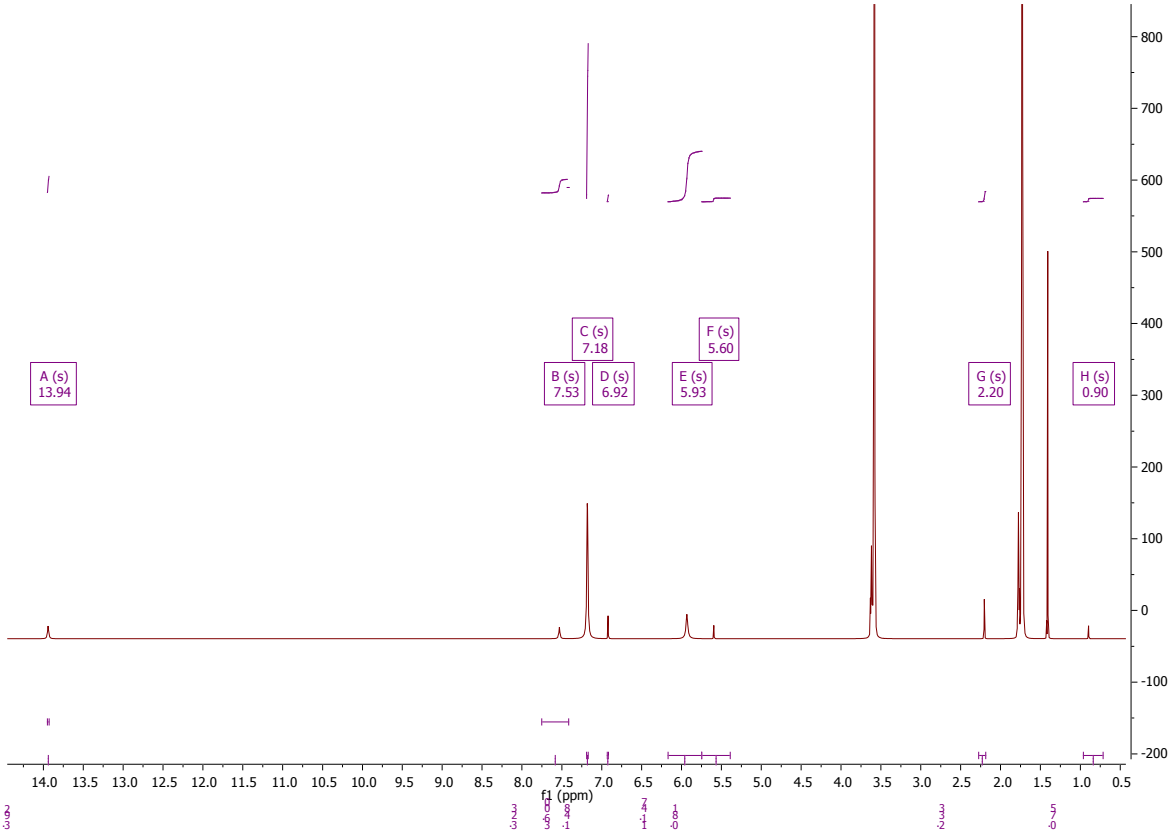

Figure S11 ^{1}H NMR spectrum of **1^{M} ($U_2I_4L^{M}$)** (C_6D_6, 500 MHz, 329 K).

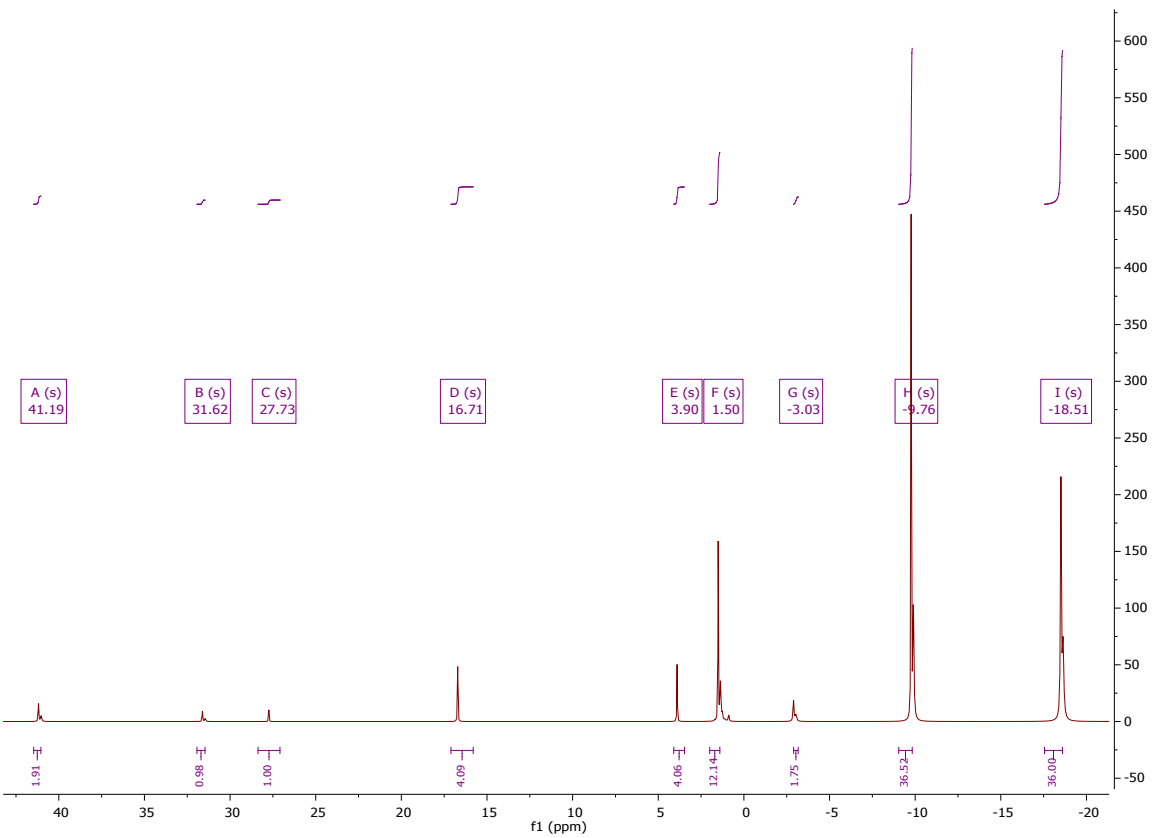

Figure S12 ^{1}H NMR spectrum of **2^{M} ($U_2N''_4L^{M}$)** (C_6D_6, 500 MHz).

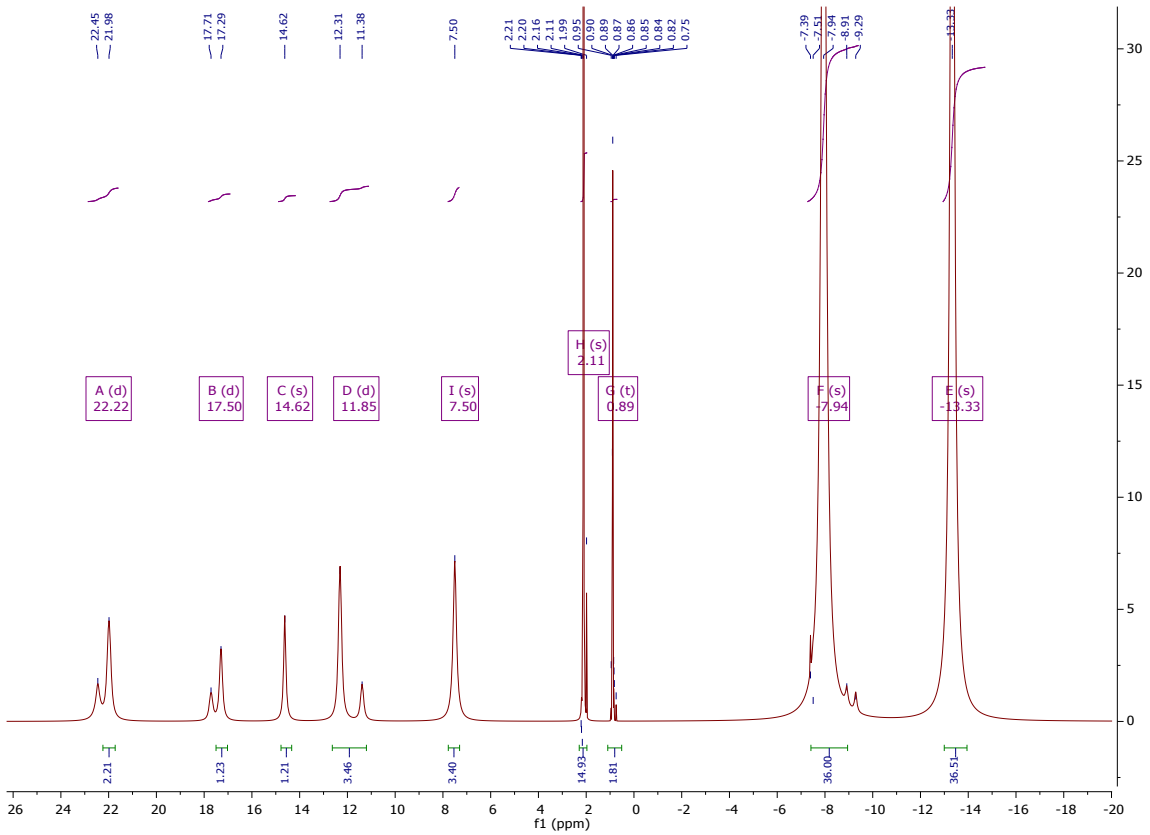

Figure S13 ^{1}H NMR spectrum of **3^{M} ($U_2N''_2L^{M}$)** (C_6D_6, 500 MHz).

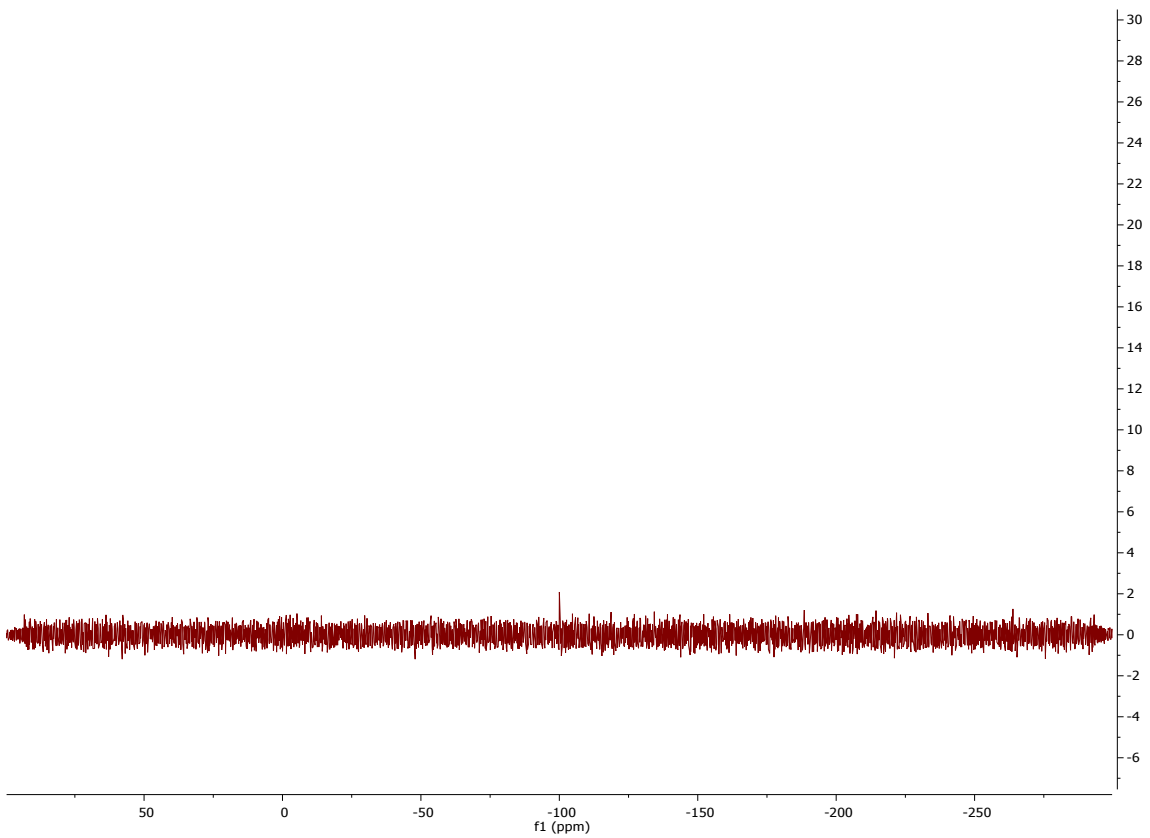

Figure S14 ^{29}Si INEPT NMR spectrum of **3^{M} ($U_2N''_2L^{M}$)** (C_6D_6, 99.4 MHz).

Selected cyclic voltammograms

Cyclic voltammograms were recorded for quiescent THF solutions using 0.1 M $[nBu_4N][BPh_4]$ as the supporting electrolyte at variable scan rates between 100 – 500 mV s^{-1}. A glassy carbon working electrode, platinum gauze counter electrode and a silver-wire quasi-reference electrode were used throughout. The voltammograms were first calibrated against decamethylcobaltocene ($CoCp^*_2$), previously dissolved in a small volume of toluene, and measured under the same conditions. They were then calibrated against the ferrocenium/ferrocene (Fc+/Fc = 0V) couple by comparison of the $E_{1/2}$ potentials of $[CoCp^*_2]^+$ /$CoCp^*_2$ and Fc^+/Fc, measured in THF against the saturated calomel electrode (SCE) taken from a different study.[1] The absence of visible redox processes in the negative region of spectra of K_4L^M suggests that the reductions seen in the cyclic voltammograms of complexes $\mathbf{1^R}$, and $\mathbf{2^R}$ are due to the redox active metal and not any ligand based reduction. Figure **S9** shows a scan of the reductive region only at 100 mVs^{-1}, overlayed on the voltammogram of $\mathbf{1^M}$ in the same region.

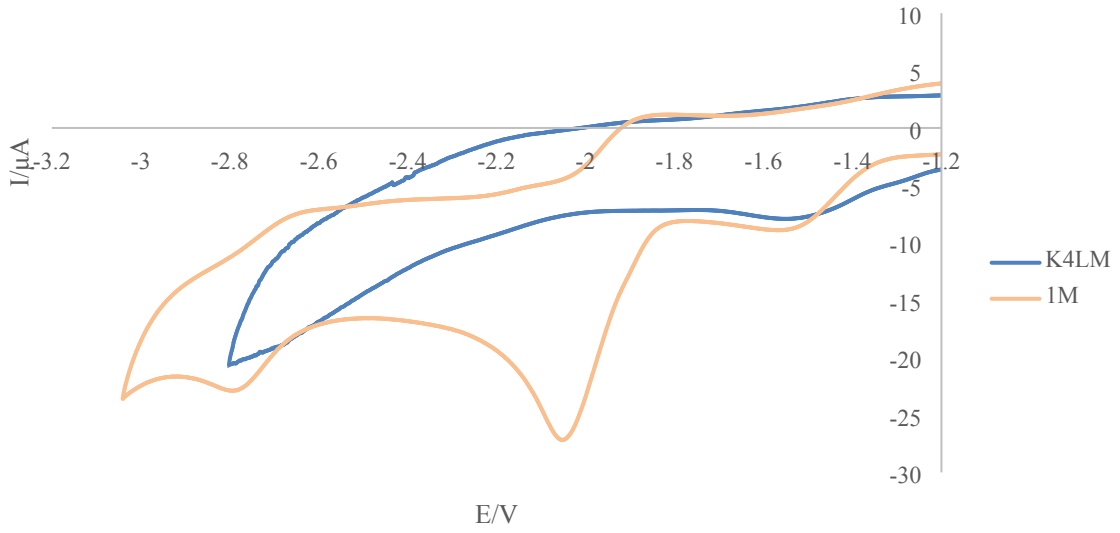

Figure S15 Cyclic voltammogram of negative region of $\mathbf{K_4L^M}$ (blue) and $\mathbf{1^M}$ (orange) in THF/$[nBu_4N][BPh_4]$ 100 mVs^{-1} scan rate.

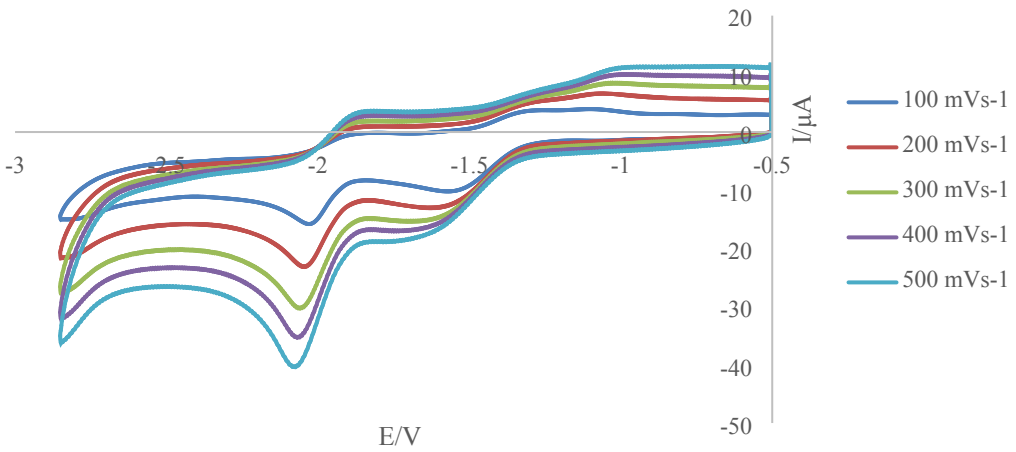

Figure S16 Cyclic voltammogram of $\mathbf{1^M}$ $\mathbf{(U_2I_4L^M)}$ in THF\$[nBu_4N][BPh_4]$. The small oxidation at -1.7V varies in size during repeated experiments and is not associated with the complex. Control experiments with supporting electrolyte and blank runs show no evidence of compound decomposition.

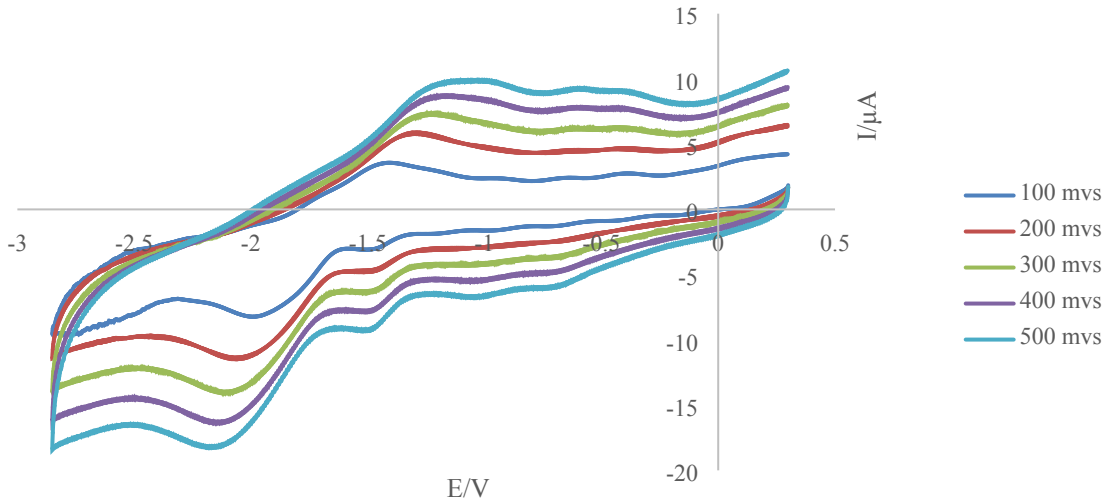

Figure S17 Cyclic voltammogram of of **2^{M} ($U_2N"_4L^{M}$)** in THF\[nBu_4N][BPh_4]. The small oxidation at -1.5V varies in size during repeated experiments and is not associated with the complex. Control experiments with supporting electrolyte and blank runs show no evidence of compound decomposition.

Crystallographic details

X-ray diffraction data for all complexes were recorded on an Excalibur Eos diffractometer at 170(2) K using Mo *Kα* radiation. All structures were solved using SHELXT [2] and least-square refined using SHELXL[3] in Olex2.[4] H atoms were treated by constrained refinement. No restraints were applied during the refinement of $\mathbf{1^{P*}}$. Disordered THF solvent in the unit cell of $\mathbf{1^{M}}$ and $\mathbf{2^{P*}}$ was heavily restrained. The structure of $\mathbf{1^{M}}$ also contained a solvent accessible void. The PLATON SQUEEZE[5] function was used to remove residual electron density of 52e− from the void, corresponding to approximately one and a third of a molecule of lattice THF per unit cell.

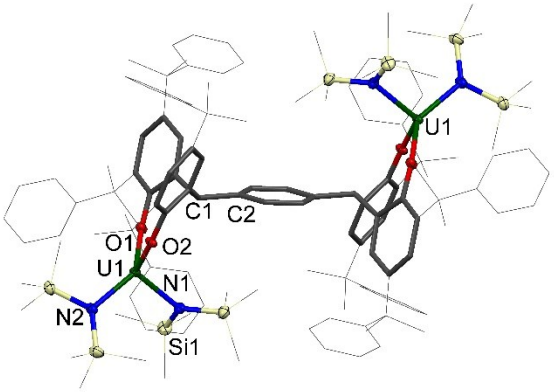

Figure S18 Solid-state structure of 2^{P*}. For clarity, all methyl groups, hydrogen atoms, and lattice solvent molecules are omitted (displacement ellipsoids are drawn at 50% probability, the remaining atoms and bonds shown as capped stick). Selected bond lengths (Å) and angles (°) for 2^{P*}: U1-O1 2.1276(19), U1-O2 2.1567(19), U1-N1 2.268(2), U1-N2 2.266(2), U1-O1-C11 148.25(17), U1-O2-C21 153.19(17).

The four coordinate uranium centres in complexes $\mathbf{2^{P}}$, $\mathbf{2^{P*}}$ and $\mathbf{2^{M}}$ all adopt distorted tetrahedral geometry. The complexes have comparable average U-O bond distances of 2.1198(13), 2.1422(19) and 2.122(4) Å respectively, which is also true of the U-N bond distances of 2.2530(16), 2.267(2) and 2.252(6) Å respectively. The slight elongation of U-O and U-N bonds in $\mathbf{2^{P*}}$ compared to $\mathbf{2^{P}}$ and $\mathbf{2^{M}}$ can be rationalised by the increased steric bulk around the metal centre in the larger tetra-aryloxide framework interfering with the sterically demanding silylamide ligands. Similarly to the iodide complexes, the U-O-C*ipso* bond angles are closer to the homoleptic uranium(IV) aryloxide, as opposed to the $I_2U(OAr)_2$ analogues, with average angles of 149.47(12)°, 150.72(17)° and 148.5(4)° for $\mathbf{2^{P}}$, $\mathbf{2^{P*}}$ and $\mathbf{2^{M}}$ respectively. The U-O bond distances are comparable to those in $U(ODtbp)_4$, as well as the *pseudo*-tetrahedral mixed aryloxo-amido uranium(IV) complexes $Et_2NU(ODtbp)_3$ and $N"_3U(ODtbp)$ with average U-O distances of 2.143(4) and 2.145(8) Å respectively. The U-N bond distances of $\mathbf{2^{R}}$ differ from the U-N distance of 2.161(5) Å exhibited by $Et_2NU(ODtbp)_3$ slightly, they agree well with the U-N bond distances exhibited by $N"_3U(ODtbp)$ and the uranium(V) complex $N"_3U(Onapth)_2$ (napth = $C_{10}H_7$) of 2.284(10) and 2.222(6) Å respectively.

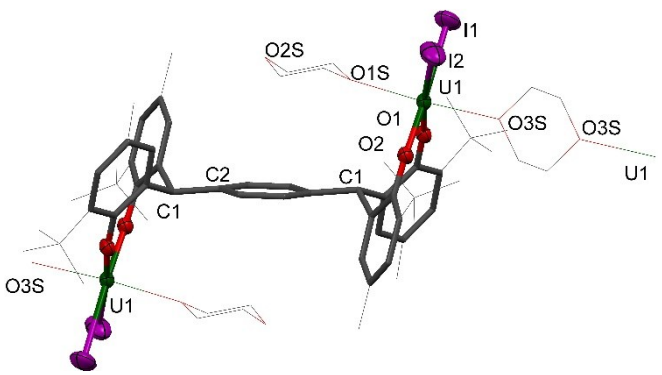

Figure S19 Solid-state structure of $\mathbf{1^{P}}$(dioxane). For clarity, all methyl groups, hydrogen atoms, and lattice solvent molecules are omitted (displacement ellipsoids are drawn at 50% probability, the remaining atoms and bonds shown as capped stick). Selected bond lengths (Å) and angles (°) for 1P: U1-O1 2.087(5), U1-O2 2.088(5), U1-I1 3.0367(7), U1-I2 3.0108(7), U1-O1-C11 157.0(5), U1-O2-C21 155.8(5).

The uranium centres in $\mathbf{1^{P}}$**(dioxane)** are in octahedral geometry, the equatorial positions are occupied by the aryloxide and iodide ligands, and the axial positions are occupied by coordinated dioxane. The exo-axial dioxanes act as a bridging ligand, linking two uranium centres intermolecularly, leading to the formation of a one-dimensional polymer in the solid state. The U-O bond lengths in $\mathbf{1^{P}}$**(dioxane)** are comparable to those of $\mathbf{1^{P}}$ at 2.088(5) and 2.1120(13) Å respectively. The U-I bond distances are slightly shorter than those of $\mathbf{1^{P}}$, 3.0238(7) and 3.1032(8) Å respectively. This may be due to the lower coordination number in $\mathbf{1^{P}}$(dioxane): fewer coordinated solvent molecules shield the uranium centre less, allowing a closer interaction with the iodide ligands. The U-O-C angles in $\mathbf{1^{P}}$(dioxane) and $\mathbf{1^{P}}$ are identical with values of 156.4(5)° and 157.1(4)°respectively.

Table S1. Crystallographic data summary for complexes $\mathbf{1^M}$ and $\mathbf{1^P}$.

Complex	$[\{UI_2(THF)_2\}_2L^M]$ ($\mathbf{1^M}$)	$[\{UI_2(THF)_3\}_2L^P]$ ($\mathbf{1^P}$)	$[\{UI_2(diox)_2\}_2L^P]$ ($\mathbf{1^P}$)
Local code	p16001-tri_sq	p15141amono	p16021d
Chemical formula	$C_{68}H_{94}I_4O_8U_2 \cdot 3(C_4H_8O)$	$C_{38}H_{55}I_2O_5U \cdot C_4H_8O$	$C_{32}H_{43}I_2O_5U \cdot 5.5(C_6H_6)$
M_r	2239.40	1155.75	1429.08
Crystal system, space group	Triclinic, *P*-1	Monoclinic, $P2_1/n$	Triclinic, *P*-1
Temperature (K)	170	170	170
a, *b*, *c* (Å)	15.8678 (6), 16.2835 (7), 21.4232 (7)	13.1203 (2), 15.46388 (16), 22.0950 (3)	13.8429 (3), 15.6696 (4), 15.8357 (5)
α, β, γ (°)	68.627 (4), 71.761 (3), 62.142 (4)	94.6475 (13)	69.881 (2), 89.136 (2), 76.2616 (19)
V (Å^3)	4488.4 (3)	4468.12 (10)	3124.73 (14)
Z	2	4	2
Radiation type	Mo *K*a	Mo *K*a	Mo *K*a
μ (mm^{-1})	5.03	5.06	3.63
Crystal size (mm)	0.29 × 0.11 × 0.02	0.29 × 0.15 × 0.13	0.51 × 0.32 × 0.13
Absorption correction	Multi-scan *CrysAlis PRO*, Agilent Technologies, Version 1.171.37.34 (release 22-05-2014 CrysAlis171 .NET) (compiled May 22 2014,16:03:01) Empirical absorption correction using spherical harmonics, implemented in SCALE3 ABSPACK scaling algorithm.	Multi-scan *CrysAlis PRO*, Agilent Technologies, Version 1.171.37.34 (release 22-05-2014 CrysAlis171 .NET) (compiled May 22 2014,16:03:01) Empirical absorption correction using spherical harmonics, implemented in SCALE3 ABSPACK scaling algorithm.	Analytical *CrysAlis PRO*, Agilent Technologies, Version 1.171.37.34 (release 22-05-2014 CrysAlis171 .NET) (compiled May 22 2014,16:03:01) Analytical numeric absorption correction using a multifaceted crystal model based on expressions derived by R.C. Clark & J.S. Reid. (Clark, R. C. & Reid, J. S. (1995). Acta Cryst. A51, 887-897) Empirical absorption correction using spherical harmonics, implemented in SCALE3 ABSPACK scaling algorithm.
T_{min}, T_{max}	0.850, 1.000	0.577, 1.000	0.991, 0.997
No. of measured, independent and observed [$I > 2s(I)$] reflections	77490, 14234, 8754	72103, 9141, 7365	58171, 14313, 10213
R_{int}	0.135	0.056	0.079
$(\sin \theta/\lambda)_{max}$ (Å^{-1})	0.575	0.625	0.649

$R[F^2 > 2\sigma(F^2)]$, $wR(F^2)$, S	0.088, 0.211, 1.03	0.053, 0.125, 1.13	0.067, 0.153, 1.03
No. of reflections	14234	9141	14313
No. of parameters	824	468	528
No. of restraints	210	91	2
$\Delta\rho_{max}$, $\Delta\rho_{min}$ (e Å^{-3})	2.51, -1.31	2.00, -1.81	1.71, -1.04
CCDC number	1478886	1478887	1478888

Table S2. Crystallographic data summary for complexes $\mathbf{1^{P*}}$, $\mathbf{2^{M}}$ and $\mathbf{2^{P}}$.

Complex	$[\{UI_2(THF)_2\}_2L^{P*}]$ ($\mathbf{1^{P*}}$)	$[\{UN''_2\}_2L^{M}]$ ($\mathbf{2^{M}}$)	$[\{UN''_2\}_2L^{P}]$ ($\mathbf{2^{P}}$)
Local code	p15180_tri	p16033_tri077	p15043
Chemical formula	$C_{60}H_{67}I_2O_4U\cdot 2(C_4H_8O)$	$C_{76}H_{134}N_4O_4Si_8U_2\cdot C_3H_7$	$C_{38}H_{67}N_2O_2Si_4U\cdot 1.89(C_{3.17}H_{3.17})$
M_r	1488.17	1911.73	1012.43
Crystal system, space group	Triclinic, *P*-1	Triclinic, *P*-1	Monoclinic, $P2_1/n$
Temperature (K)	170	170	170
a, *b*, *c* (Å)	14.4316 (3), 15.1187 (3), 16.3119 (3)	12.9013 (3), 18.8759 (4), 21.4638 (4)	13.89502 (11), 17.73106 (18), 20.67049 (18)
α, β, γ (°)	90.4479 (17), 92.5407 (16), 118.010 (2)	65.3765 (19), 88.1786 (17), 88.3450 (17)	94.3765 (8)
V (Å^3)	3137.41 (12)	4748.51 (18)	5077.81 (8)
Z	2	2	4
Radiation type	Mo *K*a	Mo *K*a	Mo *K*a
μ (mm^{-1})	3.62	3.55	3.32
Crystal size (mm)	0.33 × 0.17 × 0.09	0.32 × 0.08 × 0.02	0.54 × 0.31 × 0.13
Absorption correction	Analytical *CrysAlis PRO*, Agilent Technologies, Version 1.171.37.35 (release 13-08-2014 CrysAlis171 .NET) (compiled Aug 13 2014,18:06:01) Analytical numeric absorption correction using a multifaceted crystal model based on expressions derived by R.C. Clark & J.S. Reid. (Clark, R. C. & Reid, J. S. (1995). Acta Cryst. A51, 887-897) Empirical absorption correction using spherical harmonics, implemented in SCALE3 ABSPACK scaling algorithm.	Analytical *CrysAlis PRO*, Agilent Technologies, Version 1.171.37.35 (release 13-08-2014 CrysAlis171 .NET) (compiled Aug 13 2014,18:06:01) Analytical numeric absorption correction using a multifaceted crystal model based on expressions derived by R.C. Clark & J.S. Reid. (Clark, R. C. & Reid, J. S. (1995). Acta Cryst. A51, 887-897) Empirical absorption correction using spherical harmonics, implemented in SCALE3 ABSPACK scaling algorithm.	Multi-scan *CrysAlis PRO*, Agilent Technologies, Version 1.171.37.34 (release 22-05-2014 CrysAlis171 .NET) (compiled May 22 2014,16:03:01) Empirical absorption correction using spherical harmonics, implemented in SCALE3 ABSPACK scaling algorithm.

T_{min}, T_{max}	0.525, 0.783	0.758, 0.971	0.541, 1.000
No. of measured, independent and observed [$I > 2s(I)$] reflections	57292, 14372, 12061	85138, 16783, 11693	114610, 11616, 10176
R_{int}	0.043	0.110	0.041
$(\sin \theta/\lambda)_{max}$ (Å^{-1})	0.649	0.595	0.649
$R[F^2 > 2\sigma(F^2)]$, $wR(F^2)$, S	0.048, 0.128, 1.03	0.054, 0.096, 1.02	0.020, 0.043, 1.03
No. of reflections	14372	16783	11616
No. of parameters	603	915	558
No. of restraints	0	1	867
$\Delta\rho_{max}$, $\Delta\rho_{min}$ (e Å^{-3})	3.55, -1.87	1.07, -0.64	0.54, -0.39
CCDC number	1478889	1478890	1478891

Table S3. Crystallographic data summary for complex **2^{P}***.

Complex	[{UN"$_2$}$_2$L*] (**2^{P}***)
Local code	p15149c
Chemical formula	$C_{64}H_{87}N_2O_2Si_4U \cdot C_4H_8O \cdot C_3H_3$
M_r	1377.90
Crystal system, space group	Triclinic, *P*-1
Temperature (K)	170
a, *b*, *c* (Å)	13.1696 (3), 13.7113 (3), 20.4909 (4)
α, β, γ (°)	105.6517 (16), 103.7133 (17), 95.6555 (16)
V (Å^3)	3408.69 (12)
Z	2
Radiation type	
μ (mm^{-1})	2.50
Crystal size (mm)	0.57 × 0.17 × 0.08
Absorption correction	Analytical *CrysAlis PRO*, Agilent Technologies, Version 1.171.37.34 (release 22-05-2014 CrysAlis171 .NET) (compiled May 22 2014,16:03:01) Analytical numeric absorption

	correction using a multifaceted crystal model based on expressions derived by R.C. Clark & J.S. Reid. (Clark, R. C. & Reid, J. S. (1995). Acta Cryst. A51, 887-897) Empirical absorption correction using spherical harmonics, implemented in SCALE3 ABSPACK scaling algorithm.
T_{min}, T_{max}	0.227, 0.724
No. of measured, independent and observed [$I > 2s(I)$] reflections	70327, 13932, 12437
R_{int}	0.045
$(\sin \theta/\lambda)_{max}$ (Å^{-1})	0.625
$R[F^2 > 2\sigma(F^2)]$, $wR(F^2)$, S	0.029, 0.068, 1.06
No. of reflections	13932
No. of parameters	718
No. of restraints	15
$\Delta\rho_{max}$, $\Delta\rho_{min}$ (e Å^{-3})	1.66, -0.98
CCDC number	1478892

Selected solid-state structure drawings

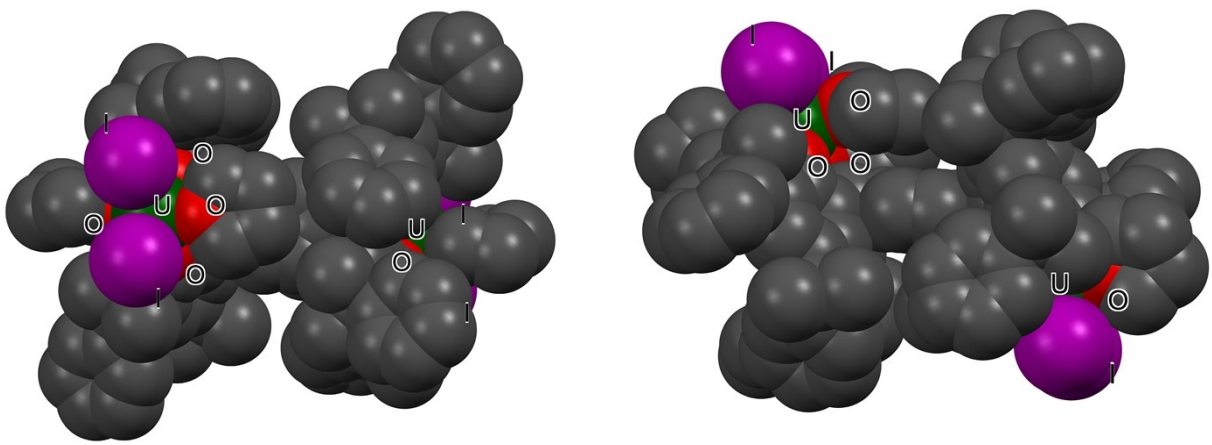

a) b)

Figure S20 Space filling drawing of (a) top and (b) side view of $U_2I_4L^{p*}$**.** Grey atoms are carbons. H and lattice solvent omitted for clarity.

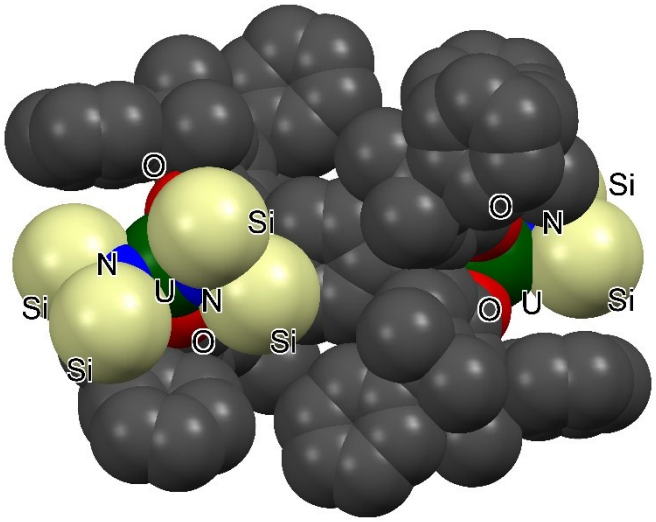

Figure S21 Space filling drawing of top view of $U_2N''_4L^{P*}$**.** Grey atoms are carbons. H and lattice solvent omitted for clarity.

References

1 Ruiz, J.; Astruc, D. *Comptes Rendus* 1998, **1**, 21-27.

2 Sheldrick, G. M. *Acta Cryst.A* 2015, **71**, 3-8.

3 Sheldrick, G. M. *Acta Cryst. C* 2015, **71**, 3-8.

4 Dolomanov, O. V.; Bourhis, L. J.; Gildea, R. J.; Howard, J. A.; Puschmann, H. *J Applied Cryst.* 2009, **42**, 339-341.

5 Spek, A. L. *Acta Cryst.C* 2015, **71**, 9-18.

